

## Effect of Hydrogen Peroxide and Sodium Alcohol Ether Sulphate on the Properties of Porous Rice Husk Ash-based Geopolymer Foam

Nurul Husna Mohd Azib<sup>1</sup>, Mohd Salahuddin Mohd Basri<sup>1,2,3\*</sup>, Mohd Zuhair Mohd Nor<sup>1</sup>, Faiqa Shazaea Mohd. Salleh<sup>1</sup>, Siti Hajar Othman<sup>1,5</sup>, Mohd Afandi P Mohammed<sup>1</sup>, Norkhairunnisa Mazlan<sup>4,5</sup>, Siti Hasnah Kamarudin<sup>6</sup> and Muhammad Hazwan Hamzah<sup>7,8</sup>

<sup>1</sup>Department of Process and Food Engineering, Faculty of Engineering, University Putra Malaysia, 43400 UPM Serdang, Selangor, Malaysia

<sup>2</sup>Laboratory of Halal Science Research, Halal Products Research Institute, Universiti Putra Malaysia (UPM), 43400 Serdang, Malaysia

<sup>3</sup>Laboratory of Biopolymer and Derivatives, Institute of Tropical Forestry and Forest Products (INTROP), Universiti Putra Malaysia, Serdang 43400, Selangor, Malaysia

<sup>4</sup>Department of Aerospace Engineering, Faculty of Engineering, University Putra Malaysia, 43400 UPM Serdang, Selangor, Malaysia

<sup>5</sup>Institute of Nanoscience and Nanotechnology (ION2), Institute of Nanoscience and Nanotechnology, Universiti Putra Malaysia, 43400 Serdang, Selangor, Malaysia

<sup>6</sup>School of Industrial Technology, Faculty of Applied Sciences, Universiti Teknologi MARA (UiTM), 40450, Shah Alam, Selangor, Malaysia

<sup>7</sup>Department of Biological and Agricultural Engineering, Faculty of Engineering, Universiti Putra Malaysia, Serdang 43400, Selangor, Malaysia

<sup>8</sup>SMART Farming Technology Research Centre, Faculty of Engineering, Universiti Putra Malaysia, Serdang 43400, Selangor, Malaysia

### ABSTRACT

Rice husk is a typical solid waste generated during rice processing, typically disposed of by combustion or landfills. One promising method for repurposing rice husk ash is as a pozzolan in

geopolymer foam. This study explores additives like hydrogen peroxide and sodium alcohol ether sulfate (SAES) to enhance the properties of porous geopolymer foam made from rice husk ash. Hydrogen peroxide is utilized as a foaming agent to enhance porosity, while SAES acts as a stabilizer to influence the structure of the foam. The foam was prepared by mixing sodium silicate, sodium hydroxide, rice husk ash, genioperl, hydrogen peroxide, and stabilizer in specific ratios. Two variables are hydrogen peroxide (0.0, 0.1, 0.2, 0.3, and 0.4 wt.%) and

#### ARTICLE INFO

##### Article history:

Received: 8 November 2023

Accepted: 5 November 2024

Published: 31 January 2025

DOI: <https://doi.org/10.47836/pjst.33.S1.04>

##### E-mail addresses:

husnaazib16@gmail.com (Nurul Husna Mohd Azib)

salahuddin@upm.edu.my (Mohd Salahuddin Mohd Basri)

zuhair@upm.edu.my (Mohd Zuhair Mohd Nor)

faiqazea@upm.edu.my (Faiqa Shazaea Mohd. Salleh)

s.hajar@upm.edu.my (Siti Hajar Othman)

afandi@upm.edu.my (Mohd Afandi P Mohammed)

norkhairunnisa@upm.edu.my (Norkhairunnisa Mazlan)

sitihasnahkam@uitm.edu.my (Siti Hasnah Kamarudin)

hazwanhamzah@upm.edu.my (Muhammad Hazwan Hamzah)

\*Corresponding author

SAES (0.0, 0.5, 1.0, 1.5, and 2.0 wt.%). The compressive strength and total porosity tests are conducted according to standards. The results show that increased hydrogen peroxide increased total porosity but decreased compressive strength. On the other hand, SAES improved the foam's structural integrity and maintained the compressive strength without significantly increasing porosity at 1.0 wt.% concentrations. The optimal total porosity and compressive strength were achieved with 0.40 wt.% hydrogen peroxide and 1.0 wt.% SAES. This study contributes to agriculture science and technology by exploring the potential use of rice husk ash-based geopolymer foam and determining the optimum formulation for its production. The findings also suggest that this foam can be utilized in various agricultural applications such as buildings, pipelines, and agriculture fields.

*Keywords:* Compressive strength, geopolymer foam, hydrogen peroxide, rice husk ash, sodium alcohol ether sulfate

---

## INTRODUCTION

Rice, a fundamental global food, contributes 21% of the world's per capita human energy and 15% of per capita protein. Rice protein, highly nutritious among cereals, contains minerals, vitamins, and fiber. Milling reduces all components except carbohydrates. Rice processing starts with pre-planting activities, including field preparation, transplanting, and harvesting (Kumar et al., 2021). Post-production involves pre-cleaning, dehusking, paddy separation, whitening, grading, weighing, and bagging. The husk separation process removes husk and bran, producing head white rice grains that are well-milled and impurity-free, containing minimal broken grains.

Rice husks, removed during milling, are protective solid coverings. In all rice-producing countries, rice husk, comprising 30%–50% organic carbon, is a readily available waste material. Rice husk composition includes cellulose (50%), lignin (25%–30%), silica (15%–20%), and moisture (10%–15%). The low bulk density of rice husk ranges from 90 kg/m<sup>3</sup> to 150 kg/m<sup>3</sup> (Singh, 2018).

Rice husk ash (RHA) is the product of rice husk incineration. Most evaporative components of rice husk are lost during burning, leaving silicates as primary residues. Ash characteristics depend on rice husk composition, temperature, and burning time. Combustion conditions significantly influence RHA chemical composition, and controlled burning is essential to retain silica in its amorphous state (Dizaji et al., 2022). Uncontrolled combustion at temperatures exceeding 700°C – 800°C produces non-reactive silica minerals like cristobalite and tridymite, making ash pulverization for pozzolanic activity economically unviable. In the construction industry, RHA applications include its use as pozzolan, filler, additive, abrasive agent, oil adsorbent, sweeping part, and suspension agent for porcelain enamels. RHA may partially substitute cement in the building industry (Pacho et al., 2024; Singh, 2018).

Geopolymers are amorphous aluminosilicate ceramic-like materials that are formed and reinforced at room temperature. It was produced using aluminosilicate sources commonly used as geopolymer binders. Alkali hydroxide and silicate solution reactions give a highly alkaline state that contributes to the polymerization process. Because of its excellent strength and environmental impact, geopolymer compounds have arisen and replaced conventional cement compounds (Komnitsas & Zaharaki, 2007; Singh & Middendorf, 2020). Production of geopolymer involves chemical reactions that convert amorphous aluminosilicates (partially or completely) into three-dimensional polymer networks. The response to geopolymerisation is exothermic. The aluminosilicate sources dissolve under a strongly alkaline medium into  $\text{SiO}_4$  and  $\text{AlO}_4$  tetrahedral units, which are subsequently involved in the polycondensation process (Celik et al., 2018). Geopolymer materials offer numerous advantages, including high resilience, fire resistance, thermal stability, excellent mechanical properties, and acid resistance (Amran et al., 2022). Low-density geopolymers find applications in thermal insulation, fire resistance, and high-temperature applications, making them potential materials (Hassan et al., 2023).

With remarkable properties, low cost, and green synthesis protocols, porous geopolymer foams have emerged as highly promising materials for various high-added-value applications (Li et al., 2023). Chemical foaming agents can prepare the cellular structure of geopolymer foam. The rice husk ash-based geopolymer foam's enhanced compressive strength and porosity make it an excellent candidate for building materials where improved thermal insulation and fire resistance are essential. For example, recent studies have demonstrated using geopolymer foams as insulation panels in energy-efficient buildings, contributing to significant reductions in heating and cooling costs (Tarek et al., 2022). In the pipeline industry, the foam's durability and resistance to chemical corrosion can extend the lifespan of pipeline coatings, reducing maintenance costs and improving safety. Additionally, its application in agriculture as a soil amendment or lightweight aggregate for green roofs can promote sustainability by reducing the environmental impact of construction activities and enhancing soil properties for better plant growth (Fatehi et al., 2021). These case studies underscore the transformative potential of our research in delivering practical, sustainable solutions across multiple sectors.

Hydrogen peroxide is a well-known alternative blowing method that creates a more uniform foam by generating gas at the molecular level. In primary media, it is thermodynamically unstable, decomposing into water and oxygen gas. The trapped gas bubbles expand within the paste, forming voids (macropores). Stabilizers, unlike catalysts, work to slow down chemical reactions. While catalysts and enzymes speed up chemical reactions, stabilizers slow them down (Yan et al., 2024). Stabilizers prevent or alter reactions like corrosion, oxidation, and separation on a molecular and chemical level. Many of these stabilizers prevent a catalyst or enzyme from performing its function. Adding a stabilizer

to the slurry improves the wet foam's stability and aids in the control of the amount of interconnected (open) porosity generated in geopolymer foam (Negri et al., 2020).

The reaction between the aluminum powder and the alkali activator or hydrogen peroxide decomposition in geopolymers allows porous structures to develop. Geopolymer foams can also be produced by gel-casting, using the geopolymerization reaction to stabilize the gas bubbles introduced by rotational mixing in the liquid slurry. Geopolymer foams have excellent physical-chemical and mechanical properties, low density, high strength, thermal stability, and good fire and chemical resistance (Coman et al., 2020; Zhao et al., 2023). The study on foam as concrete using waste materials has long been conducted. However, the study on porous geopolymer foam using rice husk ash is rather limited. Even though geopolymer material has outstanding thermal properties, limited research has been conducted on the optimum formulation for RHA-based geopolymer foam. Due to air pollution from burning rice husks in an open area, rice husks have shown great potential as waste material in producing geopolymer foam.

This study elucidates the effects of hydrogen peroxide and sodium alcohol ether sulfate (SAES) on rice husk ash-based geopolymer foam. By doing so, specific formulations that optimize compressive strength and porosity can be identified, which are crucial for expanding the applications of this material. Unlike previous studies, this study provides a comprehensive analysis of the dual role of these additives, which reveal their potential to enhance material properties for innovative uses in construction and agriculture. The optimal ratio between RHA and activated alkaline solution (AA), the amount of hydrogen peroxide, and the amount of stabilizer (sodium alcohol ether sulfate, or SAES) need to be investigated. Adding hydrogen peroxide is a blowing agent that produces a gas bubble, producing a geopolymer foam cellular structure. The purpose of adding a stabilizer is to influence the compressive strength and total porosity of the porous geopolymer foam.

Despite the promising properties of rice husk ash and its potential in geopolymer applications, research on porous geopolymer foam using rice husk ash remains limited. Most existing studies focus on single-additive systems, leaving a gap in understanding how multiple additives can enhance the material's properties. This study addresses this gap by investigating the combined effects of hydrogen peroxide and sodium alcohol ether sulfate (SAES) on the compressive strength and porosity of rice husk ash-based geopolymer foam. This dual-additive approach offers a novel strategy for optimizing material performance, providing potential for innovative construction and agriculture applications. By identifying specific formulations that optimize compressive strength and porosity, this research contributes to expanding the application scope of geopolymer foam, offering sustainable alternatives to traditional materials.

## MATERIALS AND METHODS

### Materials

Rice husk ash (RHA) was acquired from Maero Tech Sdn. Bhd., situated in Nilai 3, Negeri Sembilan. The ash underwent size reduction using a blender (MX-SM1031SSL, Panasonic, Malaysia). Sodium hydroxide (NaOH), Sodium silicates, Hydrogen peroxide ( $H_2O_2$ ), and Sodium alcohol ether sulfate (SAES) were procured from R&M Chemicals at Ever Gainful Enterprise Sdn. Bhd. in Malaysia. NaOH is available in pellet, flake, and powder formulations. This study utilized high-purity commercial-grade sodium hydroxide (NaOH) in flake form, boasting a purity level between 97% and 100%. Sodium silicates were in solution form with a purity of 98%. Sodium alcohol ether sulfate (SAES) was the hydrogen peroxide type. The SAES concentration investigated in this research ranges from 0.0 to 2.0 wt%. Genioperl P52 core-shell rubber (CSR) was acquired from Wacker Chemie AG, Germany. The synthesis process was carefully controlled to ensure the uniform distribution of hydrogen peroxide and sodium alcohol ether sulfate (SAES) within the rice husk ash-based geopolymer matrix. Preliminary trials optimized key parameters such as mixing speed, temperature, and curing time. Specifically, the stirring speed was maintained at 1100 rpm for 15 minutes to achieve a homogenous mixture, while the curing was conducted at a constant temperature of 70°C for 24 hours to ensure consistent foam structure.

### Sample Preparation

Compressive strength test samples were prepared by grinding the rice husk ash using a blender MX-SM1031SSL Panasonic, producing fine ground rice husk ash. Next, the test samples were prepared by producing the geopolymer slurry and activated alkaline (AA) solution. The AA was initially synthesized using a sodium hydroxide solution (10 M) and sodium silicate solutions in a 3.5 ratio. Subsequently, the AA solution was blended with rice husk ash (RHA) at a ratio of 0.25 to create a geopolymer slurry. The binder was introduced, along with the addition of genioperl. The geopolymer mixture was stirred gently for 15 minutes using a mechanical stirrer (Wise WiseStir Overhead Stirrer HS-30D, Witeg Labortechnik GmbH, Germany) at 1100 rpm until the solution became homogenous. After the geopolymer slurry was formed, a blowing agent (hydrogen peroxide) and stabilizing agent (SAES) were added to the mixture based on the designated composition. Amounts of hydrogen peroxide used were 0, 0.1, 0.2, 0.3, and 0.4 wt.%, while SAES were 0, 0.5, 1.0, 1.5, and 2.0 wt.%. The mixture was stirred vigorously. The samples were sealed into a mold according to the standard for the compression test (2.5 x 2.5 x 2.5 cm) and cured in an oven (Memmert Oven ULE400, MEMMERT GmbH + Co. KG, Germany) at 70°C for 24 hours. Then, the geopolymer foam (GPF) samples were stored before testing.

## Experiment Procedure

The compressive test was performed following ASTM D695 using the Instron 3382 Floor Model Universal Testing System (INSTRON ® HQ, Norwood, MA). The quantitative analysis of the total porosity of geopolymer foam was performed by calculating the value of true density and the bulk density. Density is calculated by dividing volume by weight. True density was calculated by randomly selecting the weight and volume of one sample from each group (formulation). Bulk density was calculated by the weight and volume for all samples (total 26 runs). During the experimentation, several challenges were encountered, including ensuring the stability of the foam structure, which posed a challenge, especially with varying concentrations of hydrogen peroxide. Mitigation involved optimizing sodium alcohol ether sulfate (SAES) as a stabilizing agent through iterative testing, ensuring the foam maintained its integrity throughout the curing process.

## Experimental Design

This study uses a response surface methodology (RSM) and analyzes it using MINITAB software (Minitab Statistical Software, Minitab, LLC, Pennsylvania State University). It involves two factors (hydrogen peroxide and stabilizer) and two replications for 26 runs. The design of the experiment (DOE) is shown in Table 1.

Table 1  
*Design of experiment*

Sample	Coded Factor		Uncoded Factor	
	V <sub>1</sub>	V <sub>2</sub>	V <sub>1</sub>	V <sub>2</sub>
S1	2	0	0.4	1.0
S2	0	0	0.2	1.0
S3	2	0	0.4	1.0
S4	0	0	0.2	1.0
S5	0	0	0.2	1.0
S6	0	0	0.2	1.0
S7	-1	1	0.1	1.5
S8	1	1	0.3	1.5
S9	0	0	0.2	1.0
S10	-1	-1	0.1	0.5
S11	-2	0	0.0	1.0
S12	0	0	0.2	1.0
S13	0	-2	0.2	0.0
S14	0	0	0.2	1.0
S15	-1	-1	0.1	0.5
S16	1	-1	0.3	0.5

Table 1 (continue)

Sample	Coded Factor		Uncoded Factor	
	V <sub>1</sub>	V <sub>2</sub>	V <sub>1</sub>	V <sub>2</sub>
S17	0	2	0.2	2.0
S18	0	-2	0.2	0.0
S19	-2	0	0.0	1.0
S20	1	-1	0.3	0.5
S21	0	0	0.2	1.0
S22	0	0	0.2	1.0
S23	0	0	0.2	1.0
S24	1	1	0.3	1.5
S25	-1	1	0.1	1.5
S26	0	2	0.2	2.0

## RESULTS AND DISCUSSION

### Statistical Analysis of Total Porosity and Compressive Strength Properties

Results in Table 2 show the estimated effects for total porosity, which indicates that hydrogen peroxide (V<sub>1</sub>) was the highly significant factor where P < 0.000. In contrast, the stabilizer factor (V<sub>2</sub>) was highly insignificant, with P > 0.050. The combination of V<sub>1</sub>\*V<sub>1</sub> showed significant values (P < 0.000) and affected the responses. The combination of V<sub>2</sub>\*V<sub>2</sub> and V<sub>1</sub>\*V<sub>2</sub> showed insignificant values (P > 0.050) and did not affect the responses. Significant values were observed for R<sup>2</sup> (coefficient of determination) and R<sup>2</sup> (adjusted), standing at 0.8958 and 0.8697, respectively. These results denote a substantial influence, signifying that 89.58% of the variance in the response can be attributed to the pertinent factors within the sample.

Table 2  
Estimated effects and coefficient for total porosity

Term	Notation	Coefficient	Std. error of the coefficient	P
Constant		40.1040	0.9256	0.000
Hydrogen Peroxide	V <sub>1</sub>	7.5667	0.6435	0.000
Stabilizer	V <sub>2</sub>	0.7958	0.6435	0.231
Hydrogen Peroxide * Hydrogen Peroxide	V <sub>1</sub> *V <sub>1</sub>	-2.5335	0.4657	0.000
Stabilizer * Stabilizer	V <sub>2</sub> *V <sub>2</sub>	-0.8004	0.4657	0.101
Hydrogen Peroxide * Stabilizer	V <sub>1</sub> *V <sub>2</sub>	1.7500	1.1146	0.132
R <sup>2</sup> = 89.58 percent		R <sup>2</sup> (adj) = 86.97 percent		

Regarding compressive strength, the significance of factors and their interactions was assessed with a confidence level set at 95 percent (P-value of 0.050). Notably, most

interaction effects were deemed highly insignificant when  $P > 0.050$ . The results presented in Table 3 indicate the insignificance of several factors and interaction effects, including  $V_2$ ,  $V_2*V_2$ , and  $V_1*V_2$ , as their corresponding P-values exceed 0.050. Individual factors exhibited high significance ( $P < 0.000$ ) for  $V_1$  and  $V_1*V_1$ , while insignificance was observed for  $V_2$  ( $P = 0.869$ ),  $V_2*V_2$  ( $P = 0.973$ ), and  $V_1*V_2$  ( $P = 0.949$ ). The obtained values for  $R^2$  and  $R^2$  (adjusted), namely 0.7823 and 0.7279, respectively, were considered high. It suggests that a substantial portion, specifically 78.23%, of the variance in the response within the sample can be ascribed to the independent variables.

Table 3  
Estimated effects and coefficient for compressive strength

Term	Notation	Coefficient	Std. error of coefficient	P
Constant		-0.0343	0.1139	0.766
Hydrogen Peroxide	$V_1$	0.4518	0.0792	0.000
Stabilizer	$V_2$	-0.0132	0.0792	0.869
Hydrogen Peroxide * Hydrogen Peroxide	$V_1*V_1$	0.3452	0.0573	0.000
Stabilizer * Stabilizer	$V_2*V_2$	0.0020	0.0573	0.973
Hydrogen Peroxide * Stabilizer	$V_1*V_2$	-0.0088	0.1372	0.949
$R^2 = 78.23$ percent	$R^2(\text{adj}) = 72.79$ percent			

Equations 1 and 2 represent the regression models for the total porosity and compressive strength.

$$Y_{TP} = 40.104 + 7.5667 (V_1) + 0.7958 (V_2) - 2.5335 (V_1^2) - 0.8004 (V_2^2) + 1.75 (V_1*V_2) \quad [1]$$

$$Y_{CS} = -0.0343 + 0.4518 (V_1) - 0.0132 (V_2) + 0.3452 (V_1^2) + 0.002 (V_2^2) - 0.0088 (V_1*V_2) \quad [2]$$

where  $Y_{TP}$  and  $Y_{CS}$  denote the responses, representing total porosity and compressive strength, respectively.  $V_1$  and  $V_2$  correspond to the decoded values of hydrogen peroxide and stabilizer, respectively. Utilizing regression models allows for the calculation and analysis of the influence of these factors on both total porosity and compressive strength in the context of core-shell rubber/rice husk ash-based geopolymer foam.

### Effect of Factors on Total Porosity and Compressive Strength Properties

ANOVA and regression models were employed to assess the impact of various factors on the properties of total porosity and compressive strength. Contour plots were employed for enhanced visualization, as demonstrated in Figures 1 and 2. These figures depict the influence of hydrogen peroxide ( $V_1$ ) and stabilizer ( $V_2$ ) on the responses. Both figures



indicate that higher  $V_1$  led to an increase in total porosity by up to 50 percent and an increase in compressive strength by up to 2.00 MPa. Simultaneously, elevated  $V_2$  levels resulted in a consistent total porosity of up to 50 percent and a steady compressive strength of up to 2 MPa, as depicted in both figures.

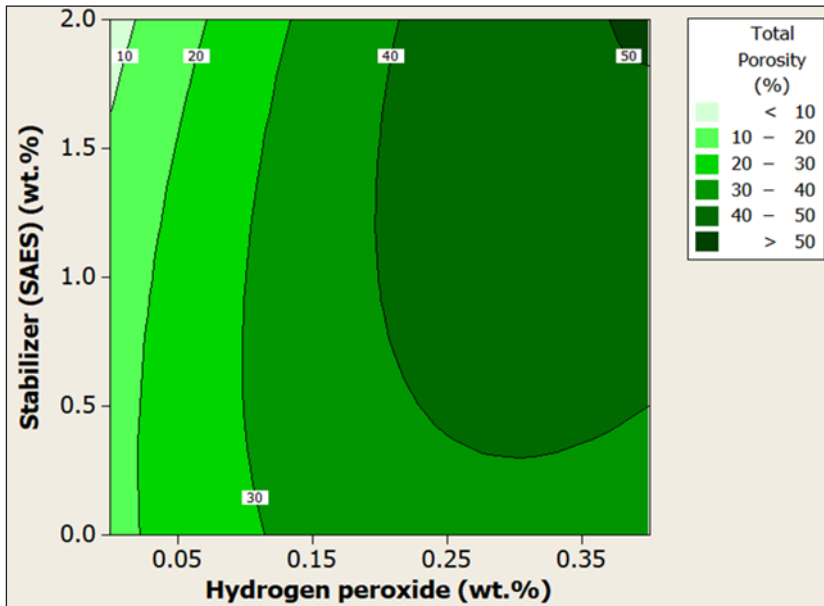


Figure 1. Contour plot for the effect of hydrogen peroxide and stabilizer on the total porosity

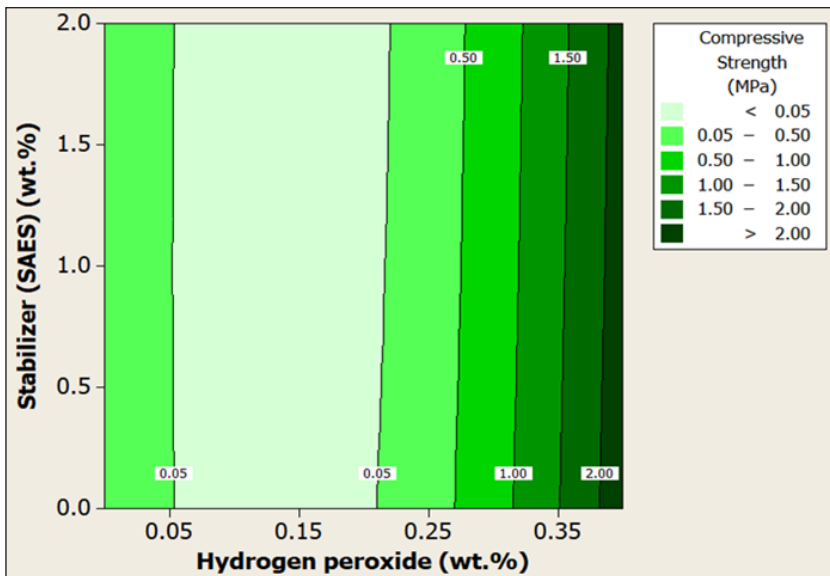


Figure 2. Contour plot for the effect of hydrogen peroxide and stabilizer on the compressive strength

From Figure 1, the total porosity of the geopolymer foam (GPF) significantly increases with increasing amounts of added hydrogen peroxide ( $V_1$ ). Adding  $V_1$  content in GPF from 0 to 0.4 wt.% at a stabilizer of 1.0 wt.% increases the total porosity from 20% to 50% region. This increment shows that  $V_1$  was significant as the pore-foaming or blowing agent (Bai et al., 2018). Increasing  $H_2O_2$  promotes endogenous gas production during preparation, resulting in larger pores and open-cell structures. It aligns with the findings of Zhang et al. (2022), who reported similar effects in polymeric foams. Unlike previous studies, the results indicate a linear increase in porosity with hydrogen peroxide concentration, suggesting a unique interaction mechanism in this composite (Posuvailo et al., 2022). Besides decreasing the total porosity when the stabilizer increases, the total porosity can be increased with the increase of the stabilizer from 0 to 0.5 wt.% at the  $H_2O_2$  of 0.25 wt.%. At the same time, the total porosity was constant with the increase of stabilizer from 0.5 to 2.0 wt.% at the  $H_2O_2$  of 0.25 wt.%.

Figures 1 and 2 illustrate the noteworthy impact of increasing hydrogen peroxide or stabilizer on porous RHA-based geopolymer foam's total porosity and compressive strength properties. It leads to a simultaneous reduction in total porosity and an enhancement in compressive strength. In Figure 2, it is evident that the compressive strength experiences a decrease as the  $H_2O_2$  content increases from 0 to 0.15 wt.%. Subsequently, compressive strength increases when the  $H_2O_2$  content is further raised from 0.15 to 0.4 wt.%. The augmentation of  $H_2O_2$  results in the formation of more air bubbles in the porous geopolymer, creating pores within the geopolymer matrix (Yan et al., 2024). This behavior is consistent with studies on foam structures where increased porosity reduces density and affects mechanical properties (Zhao et al., 2023). Hydrogen peroxide acts as a blowing agent, decomposing into oxygen and water to form pores within the material, as shown by Bhuyan et al. (2023). Adding stabilizing agents beyond 1.5 wt.% causes the air bubbles to persist and expand through coalescence, resulting in thinner walls and diminished geopolymer strengths. Notably, an increase in  $H_2O_2$  content is associated with a significant decrease in compressive strength (Ji et al., 2020). Conversely, Figure 2 indicates a consistent compressive strength of the geopolymer foam with increasing amounts of added stabilizer (SAES). It suggests that stabilizer (SAES) is an insignificant factor, and the compressive strength remains constant within the specified range of stabilizer (SAES) from 0 to 2.0 wt.% at an  $H_2O_2$  level of 0.15 wt.%.

## Optimization and Validation

Figure 3 illustrates the optimization plot showcasing the impact of different combinations of factor settings on the response. The optimization was conducted under specified parameters (hydrogen peroxide: 0.4 wt%; stabilizer: 1.0 wt%). The software predicts the optimal values for total porosity and compressive strength as 45.10 percent and 2.25 MPa, respectively,

achievable with the combination of hydrogen peroxide ( $V_1$ ) = 0.40 and stabilizer ( $V_2$ ) = 1.0. The calculated desirability of optimization is 0.83565, indicating that all parameters align with the target for achieving maximum total porosity and compressive strength properties. These optimized materials have potential applications in lightweight construction, as demonstrated by recent industrial applications (Haller et al., 2024).

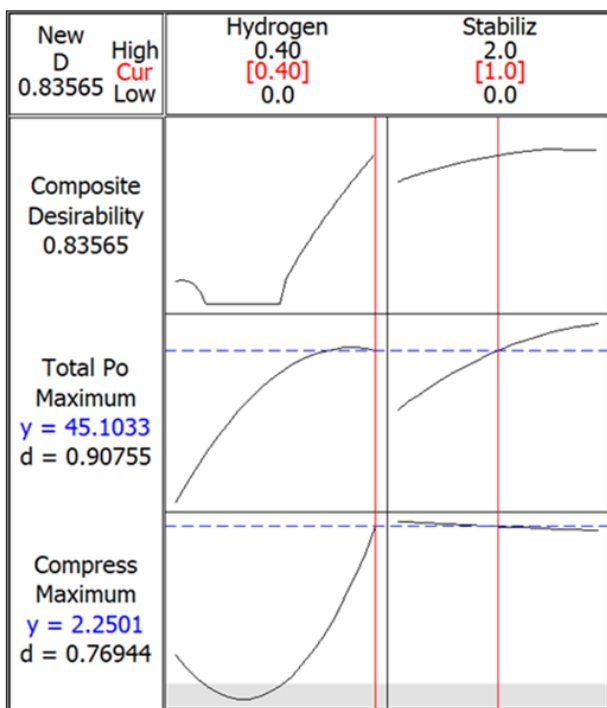


Figure 3. Optimization plot for maximum total porosity and compressive strength

Table 4

Experimental validation for the total porosity and compressive strength properties

Sample no.	Total porosity (%)			Compressive Strength (MPa)		
	Experimental value	Predicted value	Error (%)	Experimental value	Predicted value	Error (%)
SV1	45.09	45.10	0.02	2.29	2.25	1.78
SV2	44.54	45.10	1.24	2.43	2.25	8.00
	$\bar{x}$ Error		<b>0.63</b>	$\bar{x}$ Error		<b>4.89</b>

Analysis from Table 4 reveals that the average errors for total porosity and compressive strength were notably low, at 0.63% and 4.89%, respectively—well below the 15% threshold. It suggests that the regression model developed through this methodology effectively optimized the responses. In comparison to the control sample lacking hydrogen

peroxide (S19), the control sample exhibited reduced total porosity (13.31%) and increased compressive strength (0.1273 MPa).

### Material Behaviour of Sample After Compressive Strength Test

Figure 4 shows the slopes of samples S1, S9, S19 (control sample), S20 and SV2 (optimized) with brittle and ductile behavior. The samples were chosen based on best compressive strength (S1), median compressive strength (S9), sample without the addition of hydrogen peroxide (S19: control sample), poor compressive strength (S20), and optimized sample (SV2).

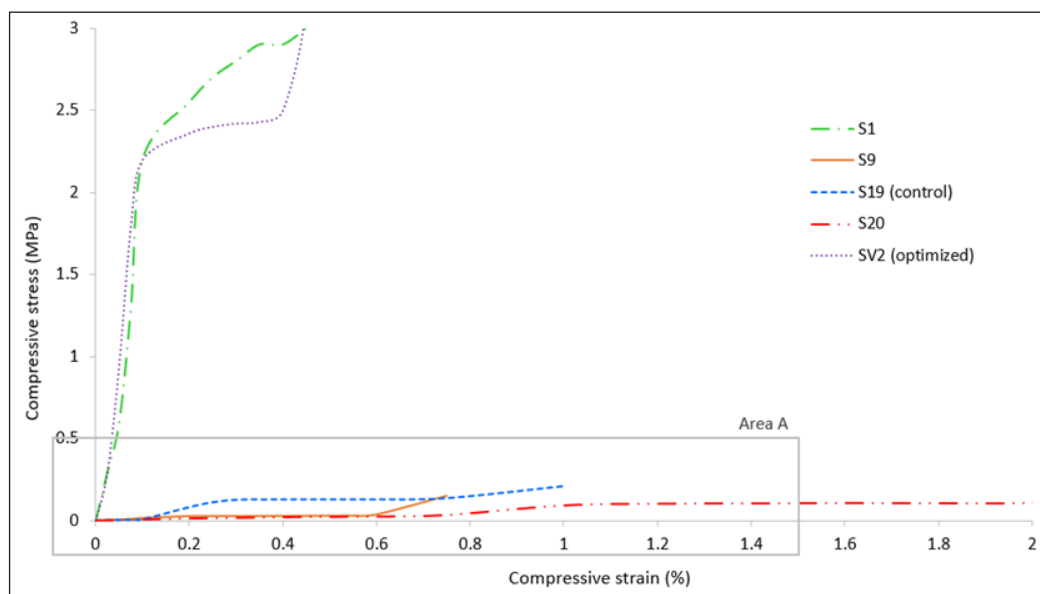


Figure 4. Stress-strain curve of samples S1, S9, S19 (control), S20, SV2 (optimized)

Figure 5 shows the enlarged area A from Figure 4. A steeper slope in a graph indicates that the material is more resilient and less prone to deformation than a gentler slope. Figure 4 shows that SV2 (optimized) (hydrogen peroxide = 0.40, stabilizer = 1.0) exhibited the steepest slope, signifying that it was the most resilient and brittle among the tested ductile samples in resisting deformation. In contrast, S20 (hydrogen peroxide = 0.30, stabilizer = 0.5) was the opposite. This result was probably due to lower hydrogen peroxide content and stabilizer. Lower hydrogen peroxide and stabilizer content lead to a gentler slope (ductile properties). This composition will cause the sample to be highly porous (a function of void content- 40.63%), so it has low compressive strength. The observed increase in brittleness with higher peroxide content has been similarly reported in recent studies by (Ransy et al., 2020).

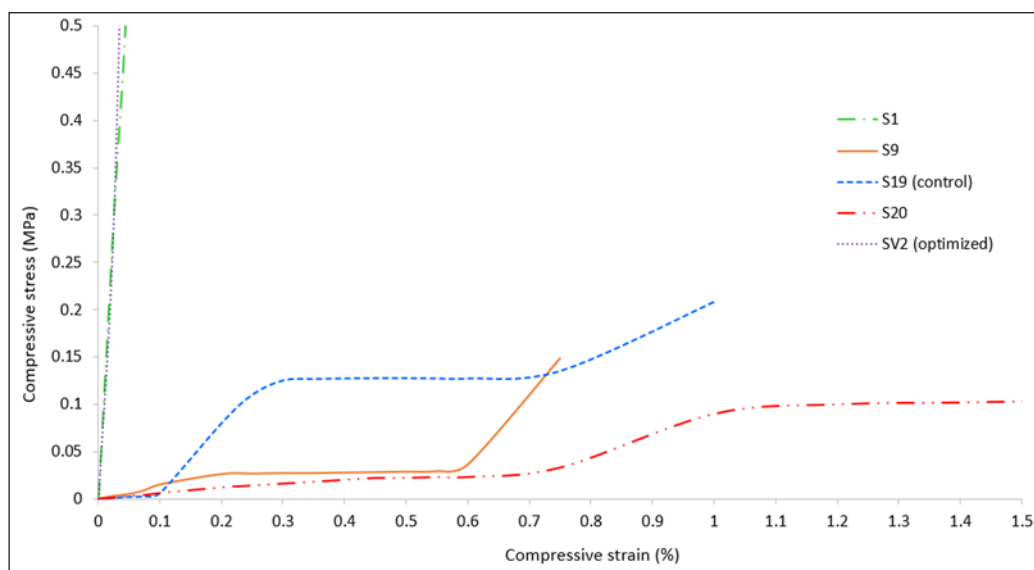


Figure 5. Enlarged area A

Although the sample without hydrogen peroxide (S19) recorded higher compressive strength (0.1273 MPa) than sample S9 (0.0253 MPa), sample S9 showed a shallower slope, which indicates that this sample was easily deformed due to lesser resilience (Funk & Dinger, 2013). This slope was due to the hydrogen peroxide and stabilizer content being at the median content (0.2% of hydrogen peroxide and 0.1% of stabilizer). It has high total porosity but low compressive strength, which leads to ductile behavior.

### Contour Plots Superimposition

The methodology employed in generating overlaid graphs for diverse response surfaces involves the integration of contour plots. This approach surpasses the conventional one-factor-at-a-time (OFAT) method, criticized for neglecting variable interactions and involvement in laborious experimental runs (Jampala et al., 2017). Figure 6 illustrates this technique, visually depicting geopolymer foam's optimal processing conditions and formulation range. The contour plot is overlaid by combining the contour plots of total porosity and compressive strength from Figures 1 and 2, respectively. The light green region signifies the total porosity and compressive strength contour area. A thorough analysis of the overlaid contour plots reveals that the optimal range for achieving the highest total porosity and compressive strength, indicated by the dark green region, falls within the ranges of 0.35–0.40 wt.% for hydrogen peroxide and 0.5–2.0 wt.% for stabilizer.

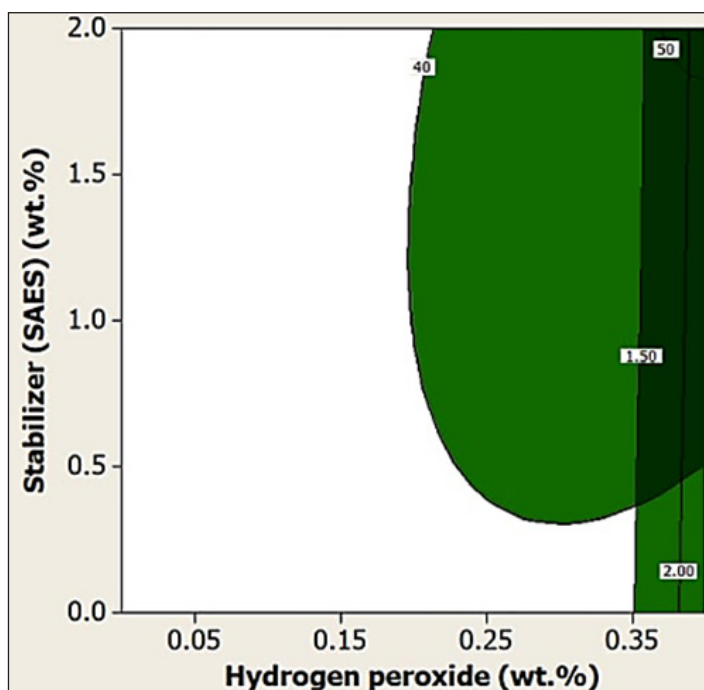


Figure 6. Optimum conditions are a function of the independent variables after the superimposition of the contour plots

## CONCLUSION

Examining the effects of hydrogen peroxide and sodium alcohol ether sulfate on the properties of porous rice husk ash-based geopolymer foam involves investigating several factors. These include determining the optimal ratio between RHA and activated alkaline solution (AA) and hydrogen peroxide and stabilizer (SAES) amounts. The results demonstrated that increasing hydrogen peroxide led to increased total porosity and decreased compressive strength due to introducing more voids. Conversely, increasing SAES reduced total porosity by stabilizing the foam structure, but higher concentrations also decreased compressive strength. The optimal balance between porosity and compressive strength was achieved with 0.4 wt.% hydrogen peroxide and 1.0 wt.% SAES. The optimal RHA-based geopolymer foam exhibits 13.3% better total porosity and foam structure when compared to the control sample. The compressive strength showed no significant changes. Due to this improvement, hydrogen peroxide and sodium alcohol ether sulfate (SAES) should be added at optimum percentages to improve the porous rice husk ash-based geopolymer foam. Additional variables such as curing time and temperature could provide further insights and should be considered. This environmentally friendly and cost-effective composite applies to agriculture, food, and construction building sectors.

## ACKNOWLEDGEMENT

The authors are grateful to the Department of Process and Food Engineering in the Faculty of Engineering, UPM, Malaysia, for the facilities to carry out the project and the NAGASE (MALAYSIA) SDN. BHD. in providing the genioperl sample.

## REFERENCES

- Amran, M., Huang, S. S., Debbarma, S., & Rashid, R. S. (2022). Fire resistance of geopolymer concrete: A critical review. *Construction and Building Materials*, 324, Article 126722. <https://doi.org/10.1016/j.conbuildmat.2022.126722>
- Bai, T., Song, Z. G., Wu, Y. G., Hu, X. D., & Bai, H. (2018). Influence of steel slag on the mechanical properties and curing time of metakaolin geopolymer. *Ceramics International*, 44(13), 15706-15713. <https://doi.org/10.1016/j.ceramint.2018.05.243>
- Bhuyan, M., Kurtulus, C., Heponiemi, A., & Luukkonen, T. (2023). Peracetic acid as a novel blowing agent in the direct foaming of alkali-activated materials. *Applied Clay Science*, 231, Article 106727. <https://doi.org/10.1016/j.clay.2022.106727>
- Celik, A., Yilmaz, K., Canpolat, O., Al-Mashhadani, M. M., Aygörmez, Y., & Uysal, M. (2018). High-temperature behavior and mechanical characteristics of boron waste additive metakaolin based geopolymer composites reinforced with synthetic fibers. *Construction and Building Materials*, 187, 1190-1203. <https://doi.org/10.1016/j.conbuildmat.2018.08.062>
- Coman, V., Teleky, B. E., Mitrea, L., Martău, G. A., Szabo, K., Călinoiu, L. F., & Vodnar, D. C. (2020). Bioactive potential of fruit and vegetable wastes. *Advances in Food and Nutrition Research*, 91, 157-225. <https://doi.org/10.1016/bs.afnr.2019.07.001>
- Dizaji, H. B., Zeng, T., Hölzig, H., Bauer, J., Klöß, G., & Enke, D. (2022). Ash transformation mechanism during combustion of rice husk and rice straw. *Fuel*, 307, Article 121768. <https://doi.org/10.1016/j.fuel.2021.121768>
- Fatehi, H., Ong, D. E., Yu, J., & Chang, I. (2021). Biopolymers as green binders for soil improvement in geotechnical applications: A review. *Geosciences*, 11(7), Article 291. <https://doi.org/10.3390/geosciences11070291>
- Funk, J. E., & Dinger, D. R. (2013). *Predictive process control of crowded particulate suspensions: Applied to ceramic manufacturing*. Springer.
- Haller, T., Beuntner, N., & Thienel, K. C. (2024). Optimized building envelope: Lightweight concrete with integrated steel framework. *Materials*, 17(6), Article 1278. <https://doi.org/10.3390/ma17061278>
- Hassan, A., Arif, M., Shariq, M., Alomayri, T., & Pereira, S. (2023). Fire resistance characteristics of geopolymer concrete for environmental sustainability: A review of thermal, mechanical and microstructure properties. *Environment, Development and Sustainability*, 25(9), 8975-9010. <https://doi.org/10.1007/s10668-022-02495-0>
- Jampala, P., Tadikamalla, S., Preethi, M., Ramanujam, S., & Uppuluri, K. B. (2017). Concurrent production of cellulase and xylanase from *Trichoderma reesei* NCIM 1186: Enhancement of production by desirability-based multi-objective method. *3 Biotech*, 7(1), Article 14. <https://doi.org/10.1007/s13205-017-0607-y>

- Ji, Z., Li, M., Su, L., & Pei, Y. (2020). Porosity, mechanical strength and structure of waste-based geopolymer foams by different stabilizing agents. *Construction and Building Materials*, 258, Article 119555. <https://doi.org/10.1016/j.conbuildmat.2020.119555>
- Komnitsas, K., & Zaharaki, D. (2007). Geopolymerisation: A review and prospects for the minerals industry. *Minerals Engineering*, 20(14), 1261-1277. <https://doi.org/10.1016/j.mineng.2007.07.011>
- Kumar, N., Chhokar, R., Meena, R., Kharub, A., Gill, S., Tripathi, S., Gupta, O., Mangrauthia, S., Sundaram, R., & Sawant, C. (2021). Challenges and opportunities in productivity and sustainability of rice cultivation system: a critical review in Indian perspective. *Cereal Research Communications*, 50, 573–601. <https://doi.org/10.1007/s42976-021-00214-5>
- Li, X., Shao, J., Zheng, J., Bai, C., Zhang, X., Qiao, Y., & Colombo, P. (2023). Fabrication and application of porous materials made from coal gangue: A review. *International Journal of Applied Ceramic Technology*, 20(4), 2099-2124. <https://doi.org/10.1111/ijac.14359>
- Negri, C., Ricci, M., Zilio, M., D'Imporzano, G., Qiao, W., Dong, R., & Adani, F. (2020). Anaerobic digestion of food waste for bio-energy production in China and Southeast Asia: A review. *Renewable and Sustainable Energy Reviews*, 133, Article 110138. <https://doi.org/10.1016/j.rser.2020.110138>
- Pacho, J. K. M., Florencondia, N., & Aduna, E. J. R. (2024). Evaluating the optical properties of philippine rice hull ash as a potential alternative to calcium carbonate filler for paints. *Iconic Research and Engineering Journals*, 7(11), 477-483.
- Posuvailo, V., Kovalchuk, I., & Ivashenko, I. (2022). Influence of hydrogen peroxide on the composition and porosity of oxide-ceramic coatings on alloys of the Al–Si–Cu and Al–Cu–Mg systems. *Materials Science*, 57(6), 894-899. <https://doi.org/10.1007/s11003-022-00619-5>
- Ransy, C., Vaz, C., Lombès, A., & Bouillaud, F. (2020). Use of H<sub>2</sub>O<sub>2</sub> to cause oxidative stress, the catalase issue. *International journal of molecular sciences*, 21(23), Article 9149. <https://doi.org/10.3390/ijms21239149>
- Singh, B. (2018). Rice husk ash. In R. Siddique & P. Cachim (Eds.) *Waste and supplementary cementitious materials in concrete* (pp. 417-460). Woodhead Publishing. <https://doi.org/10.1016/B978-0-08-102156-9.00013-4>
- Singh, N. B., & Middendorf, B. (2020). Geopolymers as an alternative to Portland cement: An overview. *Construction and Building Materials*, 237, Article 117455. <https://doi.org/10.1016/j.conbuildmat.2019.117455>
- Tarek, D., Ahmed, M., Hussein, H. S., Zeyad, A. M., Al-Enizi, A. M., Yousef, A., & Ragab, A. (2022). Building envelope optimization using geopolymer bricks to improve the energy efficiency of residential buildings in hot arid regions. *Case Studies in Construction Materials*, 17, Article e01657. <https://doi.org/10.1016/j.cscm.2022.e01657>
- Yan, D., Shi, Y., Zhang, Y., Wang, W., Qian, H., Chen, S., Liu, Y., & Ruan, S. (2024). A comparative study of porous geopolymers synthesized by pre-foaming and H<sub>2</sub>O<sub>2</sub> foaming methods: Strength and pore structure characteristics. *Ceramics International*, 50(10), 17807-17817. <https://doi.org/10.1016/j.ceramint.2024.02.270>



- Zhang, X., Zhang, X., Li, X., Tian, D., Ma, M., & Wang, T. (2022). Optimized pore structure and high permeability of metakaolin/fly-ash-based geopolymer foams from Al<sup>-</sup>and H<sub>2</sub>O<sub>2</sub>-sodium oleate foaming systems. *Ceramics International*, 48(13), 18348-18360. <https://doi.org/10.1016/j.ceramint.2022.03.094>
- Zhao, J., Trindade, A. C. C., Liebscher, M., de Andrade Silva, F., & Mechtcherine, V. (2023). A review of the role of elevated temperatures on the mechanical properties of fiber-reinforced geopolymer (FRG) composites. *Cement and Concrete Composites*, 137, Article 104885. <https://doi.org/10.1016/j.cemconcomp.2022.104885>